Hindawi Publishing Corporation
Mathematical Problems in Engineering
Volume 2012, Article ID 832836, 21 pages
doi:10.1155/2012/832836

Research Article

Data-Driven Adaptive Observer for Fault Diagnosis

Shen Yin,[1] Xuebo Yang,[1] and Hamid Reza Karimi[2]

[1] *Research Institute of Intelligent Control and Systems, Harbin Institute of Technology, Harbin 150001, China*
[2] *Faculty of Engineering and Science, University of Agder, 4898 Grimstad, Norway*

Correspondence should be addressed to Shen Yin, shen.yin2011@gmail.com

Received 25 June 2012; Accepted 12 August 2012

Academic Editor: Bo Shen

This paper presents an approach for data-driven design of fault diagnosis system. The proposed fault diagnosis scheme consists of an adaptive residual generator and a bank of isolation observers, whose parameters are directly identified from the process data without identification of complete process model. To deal with normal variations in the process, the parameters of residual generator are online updated by standard adaptive technique to achieve reliable fault detection performance. After a fault is successfully detected, the isolation scheme will be activated, in which each isolation observer serves as an indicator corresponding to occurrence of a particular type of fault in the process. The thresholds can be determined analytically or through estimating the probability density function of related variables. To illustrate the performance of proposed fault diagnosis approach, a laboratory-scale three-tank system is finally utilized. It shows that the proposed data-driven scheme is efficient to deal with applications, whose analytical process models are unavailable. Especially, for the large-scale plants, whose physical models are generally difficult to be established, the proposed approach may offer an effective alternative solution for process monitoring.

1. Introduction

During the last two decades, diagnostic observers and parity space-based fault detection and isolation (FDI) schemes for linear time invariant (LTI) systems are intensively studied [1–6]. The core of the parity space FDI technique is, based on state space representation of the system, construction of residual generator by means of the so-called parity vector, which is the null space of the observability matrix. As pointed out in Ding [6], the design of an observer-based residual generator can be equivalently formulated as a similar problem.

Since the majority of observer and parity space-based FDI schemes involve rigorous development of process models based on the first principles, later identification techniques that extracts transfer function [7] or state space model become a necessary step prior to

the design. For this purpose, subspace identification methods (SIM) that identify the complete state space matrices have been successfully implemented see Overschee and Moor [8], Favoreel et al. [9], and Qin [10]. Provided the process model is known *a priori*, observer and parity space-based FDI systems can be designed with a large number of applications [11–13]. The approaches of filtering and control for such complex systems have been well studied in the literature; see Shen et al. [14], Shen et al. [15], and Dong et al. [16], Dong et al. [17]. Recently, an alternative data-driven approach has been proposed that does not require the identification of complete set of process model but only the so-called primary form of the residual generator from the process data; see Ding et al. [18]. Based on it, the advanced observer-based FDI system can be designed in an efficient way [19–23]. Thanks to its simple forms and less requirements on the design and engineering efforts, the data-driven FDI approach becomes more efficient in many industry sectors, especially for large-scale industry applications [24]. Recent survey given by Ding et al. [22, 23] provided the reader with a comprehensive overview on the basic and advanced data-driven FDI schemes.

Our study is motivated by the aforementioned data-driven FDI approach, in that we also recognize the wide existence of systems with uncertain or normal variation parameters in practice, which have not been paid enough attention in research study. Extension of the data-driven FDI scheme to such processes will improve the safety and reliability of these applications and further reduce the complexity to perform FDI especially on the large-scale systems. For this purpose, a data-driven fault diagnosis approach was proposed in this paper, in which the issues of fault isolation and threshold setting were studied to complete the earlier work given by Ding et al. [19, 20]. The structure of the fault diagnosis scheme consists of an adaptive residual generator and a bank of isolation observers, whose parameters are directly updated from the plant data with standard adaptive technique to cope with normal variations in the process. The threshold for fault detection can be determined either analytically or by probability density function estimation technique. When a fault is detected, the fault isolation scheme is activated, in which each isolation observer indicates the occurrence of a particular type of fault in the process. Fault isolation is successfully achieved when all the isolation indices, except the one responsible for the fault, exceed the thresholds. For the realization of the isolation scheme, the standard projection algorithm is implemented [25, 26]. The sufficient condition of fault isolability is also analyzed in this work.

The rest of the paper is organized as follows. In Section 2, the mathematical preliminaries and problem formulation are presented. Section 3 addresses the theoretical core of the proposed fault diagnosis scheme, in which both fault detection and isolation issues will be analyzed in detail. In Section 4, the simulation of laboratory-scale three-tank system is used to illustrate the performance of the proposed scheme. The paper ends with concluding remarks in the last section.

2. Preliminaries and Problem Formulation

2.1. Preliminaries of Model-Based Residual Generator

Consider a discrete-time LTI system which is described by

$$x_{k+1} = Ax_k + Bu_k, \tag{2.1}$$

$$y_k = Cx_k, \tag{2.2}$$

where $x_k \in \mathcal{R}^n$, $u_k \in \mathcal{R}^l$, and $y_k \in \mathcal{R}^m$ represent the vector of state variables and process input and output, respectively. A, B, and C are system matrices with appropriate dimensions. Reformulate (2.1)-(2.2) into

$$Z = \begin{bmatrix} Y \\ U \end{bmatrix} = \begin{bmatrix} \Gamma_s & H_{s,u} \\ 0 & I \end{bmatrix} \begin{bmatrix} X_i \\ U \end{bmatrix} \in \mathcal{R}^{(s+1)(m+l)\times N}, \tag{2.3}$$

where $X_i = [x_i \; x_{i+1} \; \cdots \; x_{i+N-1}] \in \mathcal{R}^{n\times N}$, $U = [u_{s,k} \; \cdots \; u_{s,k+N-1}] \in \mathcal{R}^{(s+1)l\times N}$, $Y = [y_{s,k} \; \cdots \; y_{s,k+N-1}] \in \mathcal{R}^{(s+1)m\times N}$, and

$$y_{s,k} = \begin{bmatrix} y_{k-s} \\ \vdots \\ y_k \end{bmatrix}, \quad u_{s,k} = \begin{bmatrix} u_{k-s} \\ \vdots \\ u_k \end{bmatrix}, \quad \Gamma_s = \begin{bmatrix} C \\ CA \\ \vdots \\ CA^s \end{bmatrix}, \quad H_{s,u} = \begin{bmatrix} 0 & 0 & \cdots & 0 \\ CB & 0 & \cdots & 0 \\ \vdots & \ddots & \ddots & \vdots \\ CA^{s-2}B & \cdots & CB & 0 \end{bmatrix}, \tag{2.4}$$

and $s(\geq n)$ and $N(\gg s)$ are integers. On the assumption of known A, B, and C, the design of a parity space-based residual generator consists in solving

$$\alpha_s \Gamma_s = 0, \tag{2.5}$$

for the so-called parity vector $\alpha_s[\alpha_{s,0} \; \alpha_{s,1} \; \cdots \; \alpha_{s,s}] \in \mathcal{R}^{1\times(s+1)m}$. The design of an observer-based residual generator is achieved by solving the so-called Luenberger equations

$$TA - A_z T = LC, \qquad c_z T = gC, \qquad B_z = TB, \tag{2.6}$$

$$A_z \in \mathcal{R}^{s\times s}, \qquad T \in \mathcal{R}^{s\times n}, \qquad c_z \in \mathcal{R}^{1\times s}, \qquad g \in \mathcal{R}^{1\times m} \tag{2.7}$$

for A_z (should be stable), B_z, c_z, g, L together with a transformation matrix T. It follows then the construction of the parity space-based residual generator

$$r_k = \alpha_s\left(y_{s,k} - H_{s,u}u_{s,k}\right), \tag{2.8}$$

and the observer-based residual generation

$$z_{k+1} = A_z z_k + B_z u_k + L y_k \in \mathcal{R}^s, \tag{2.9}$$

$$r_k = g y_k - c_z z_k \in \mathcal{R}. \tag{2.10}$$

In the above equations, r_k is called residual signal and s the order of the parity space or the observer-based residual generator. The following lemma given by Ding [6] describes the one-to-one mapping between the parity vector and the solutions of Luenberger equations.

Lemma 2.1 (see Ding [6]). *Given any parity vector* $\alpha_s = [\alpha_{s,0}\ \alpha_{s,1}\ \cdots\ \alpha_{s,s}]$, *with* $\alpha_{s,i} \in \mathcal{R}^{1\times m}$, $i = 0, 1, \ldots, s$ *and process model* (2.1)-(2.2), *then*

$$A_z = \begin{bmatrix} 0 & 0 & \cdots & 0 \\ 1 & 0 & \cdots & 0 \\ \vdots & \ddots & \ddots & \vdots \\ 0 & \cdots & 1 & 0 \end{bmatrix} \in \mathcal{R}^{s\times s}, \qquad L = -\begin{bmatrix} \alpha_{s,0} \\ \alpha_{s,1} \\ \vdots \\ \alpha_{s,s-1} \end{bmatrix}, \qquad T = \begin{bmatrix} \alpha_{s,1} & \alpha_{s,2} & \cdots & \alpha_{s,s} \\ \alpha_{s,2} & \cdots & \alpha_{s,s} & 0 \\ \vdots & \ddots & \ddots & \vdots \\ \alpha_{s,s} & 0 & \cdots & 0 \end{bmatrix} \begin{bmatrix} C \\ CA \\ \vdots \\ CA^{s-1} \end{bmatrix}, \tag{2.11}$$

$$c_z = \begin{bmatrix} 0 & \cdots & 0 & 1 \end{bmatrix} \in \mathcal{R}^{1\times s}, \qquad g = \alpha_{s,s} \in \mathcal{R}^{1\times m}, \tag{2.12}$$

solve the Luenberger equations (2.6).

2.2. Preliminaries of Data-Driven Residual Generator Design

It is assumed that system matrices A, B, and C and system order n are *unknown a priori*; Ding et al. [19, 20] proposed an approach for data-driven design of observer-based residual generator, which briefly consists of two algorithms, that is,

(i) *Algorithm D2PS* (from data to parity subspace),

(ii) *Algorithm PS2DO* (from parity vector to diagnostic observer (DO)).

Algorithm 2.2. D2PS (from data to parity subspace).

Step 1. Generate data sets Z and construct $(1/N)ZZ^T$.
Step 2. Compute the SVD of $(1/N)ZZ^T$

$$\begin{gathered} \frac{1}{N}ZZ^T = U_z \begin{bmatrix} \Sigma_{z,1} & 0 \\ 0 & \Sigma_{z,2} \end{bmatrix} U_z^T, \\ U_z = \begin{bmatrix} U_{z,11} & U_{z,12} \\ U_{z,21} & U_{z,22} \end{bmatrix}, \qquad \Sigma_{z,2} = 0 \in \mathcal{R}^{((s-1)m-n)\times((s-1)m-n)}, \\ U_{z,11} \in \mathcal{R}^{(s+1)m\times((s+1)l+n)}, \qquad U_{z,12}^T \in \mathcal{R}^{((s+1)m-n)\times(s+1)m}. \end{gathered} \tag{2.13}$$

Step 3. Set $\Gamma_s^{\perp} = U_{z,12}^T$, $\Gamma_s^{\perp} H_{s,u} = -U_{z,22}^T$.

Note that any row of matrix $\Gamma_s^{\perp}$ is a parity vector. For a system with multiple output ($m > 1$), $(s+1)m$ may be significantly larger than n. In order to reduce the online computation, an order reduction algorithm is given by Ding et al. [19, 20] to achieve a reduced order $s \le n$. For multiple output systems, s may be significantly smaller than n.

Algorithm 2.3. PS2DO (from parity vector to DO).

Step 1. Select $\alpha_s \in \Gamma_s^{\perp}$ and corresponding row $\beta_s \in \Gamma_s^{\perp} H_{s,u}$ and form them as

$$\begin{aligned} \alpha_s &= \begin{bmatrix} \alpha_{s,0} & \alpha_{s,1} & \cdots & \alpha_{s,s} \end{bmatrix}, \quad \alpha_{s,i} \in \mathcal{R}^{1\times m}, \\ \beta_s &= \begin{bmatrix} \beta_{s,0} & \beta_{s,1} & \cdots & \beta_{s,s} \end{bmatrix}, \quad \beta_{s,i} \in \mathcal{R}^{1\times l}. \end{aligned} \tag{2.14}$$

Step 2. Set A_z, c_z, L, g according to (2.11)-(2.12) and $B_z^T = [\beta_{s,0}^T \cdots \beta_{s,s-1}^T]$.
Step 3. Construct the DO according to (2.9)-(2.10).

2.3. Problem Formulation

So far in our study, the data-driven fault detection scheme has been developed for LTI systems. However, The wide existence of systems with uncertain or normal variation parameters has not been considered enough in the literatures. In order to develop an efficient data-driven fault diagnosis scheme for such systems, it is necessary to

(i) propose an efficient residual generator to deal with normal parameter variations in the process,

(ii) determine proper threshold for fault detection purpose,

(iii) develop related fault isolation strategy to complete the diagnosis task.

Without loss of generality, in the remaining part of this paper, the parameter variation rate is assumed bound in term of l^2-norm. In addition, the persistent excitation condition for identification methods is assumed to be satisfied.

3. Data-Driven Design of Fault Diagnosis Scheme

3.1. Adaptive Residual Generator-Based Fault Detection Scheme

According to Lemma 2.1, the system (2.1)-(2.2) can be represented in following form:

$$z_{k+1} = \overline{A}_z z_k + Q(u_k, y_k)\theta, \tag{3.1}$$

where $z_k = Tx_k$, $\overline{A}_z = A_z - L_0 c_z$, L_0 is a design parameter vector to ensure that the eigenvalues of $\overline{A}_z$ lie in the unit circle and

$$\begin{gathered} Q(u_k, y_k) = \left[\overline{Q}(u_k, y_k) \;\; L_0 y_k^T\right] \in \mathcal{R}^{s\times[s(m+l)+m]}, \\ \overline{Q}(u_k, y_k) = \left[\mathcal{U}_k \;\; \mathcal{Y}_k\right] \in \mathcal{R}^{s\times s(m+l)}, \\ \mathcal{U}_k = \left[u_{1,k} \times I_{s\times s} \;\; \cdots \;\; u_{l,k} \times I_{s\times s}\right], \qquad \mathcal{Y}_k = \left[y_{1,k} \times I_{s\times s} \;\; \cdots \;\; y_{m,k} \times I_{s\times s}\right], \\ \theta = \begin{bmatrix} \overline{\theta} \\ g^T \end{bmatrix} \in \mathcal{R}^{s(m+l)+m}, \qquad \overline{\theta} = \begin{bmatrix} \mathrm{col}(B_z) \\ \mathrm{col}(L) \end{bmatrix} \in \mathcal{R}^{s(m+l)}, \end{gathered} \tag{3.2}$$

with col(•) denotes a column-wise reordering of a matrix; that is,

$$P = \left[p_1 \;\; \cdots \;\; p_\alpha\right] \in \mathcal{R}^{\beta\times\alpha}, \qquad \mathrm{col}(P) = \begin{bmatrix} p_1 \\ \vdots \\ p_\alpha \end{bmatrix} \in \mathcal{R}^{\beta\alpha\times 1}. \tag{3.3}$$

In the following study, set $L_0 = 0$ for the purpose of simplicity.

Note that in (3.1) the system matrices A, B, and C are integrated into vector θ, and the input and output signals are included in $Q(u_k, y_k)$. Any parameter variation in the original system can be reflected through the parameter variation rate defined as $\Delta_k = \theta_{k+1} - \theta_k$, which is bounded by

$$\|\Delta_k\| \leq v, \tag{3.4}$$

where $\|\bullet\|$ denotes l^2-norm. Let us firstly consider the basic case, that is, a constant parameter θ; the adaptive residual generator is stated in the following theorem.

Theorem 3.1. *Given the following adaptive residual generator which consists of three subsystems.*

(i) Residual generator:

$$\hat{z}_{k+1} = \overline{A}_z \hat{z}_k + Q(u_k, y_k)\hat{\theta}_k + V_{k+1}\left(\hat{\theta}_{k+1} - \hat{\theta}_k\right), \tag{3.5}$$

$$r_k = \hat{g}_k y_k - c_z \hat{z}_k. \tag{3.6}$$

(ii) Auxiliary filter

$$V_{k+1} = \overline{A}_z V_k + Q(u_k, y_k) \in \mathcal{R}^{s\times[s(m+l)+m]}, \tag{3.7}$$

$$\varphi_k = c_z V_k - \begin{bmatrix} 0 & \cdots & 0 & y_k^T \end{bmatrix} \in \mathcal{R}^{s(m+l)+m}. \tag{3.8}$$

(iii) Parameter estimator

$$\hat{\theta}_{k+1} = \gamma_k \varphi_k^T r_k + \hat{\theta}_k \in \mathcal{R}^{s(m+l)+m}, \tag{3.9}$$

$$\gamma_k = \frac{\mu}{\delta + \varphi_k \varphi_k^T}, \quad \delta > 0,\ 0 < \mu < 2, \tag{3.10}$$

$$\hat{\theta}_k = \begin{bmatrix} \hat{\bar{\theta}}_k \\ (\hat{g}_k)^T \end{bmatrix}, \quad \hat{\bar{\theta}}_k \in \mathcal{R}^{s(m+l)},\ \hat{g}_k \in \mathcal{R}^{1\times m}. \tag{3.11}$$

it follows that the adaptive residual generator is stable and in the fault-free case the residual signal satisfies

$$\lim_{k\to\infty} r_k = 0. \tag{3.12}$$

Moreover, if the persistent excitation condition is satisfied; that is, there exist positive constants β_1, β_2 and integer Π such that for all k

$$0 < \beta_1 I \leq \sum_{i=k}^{k+\Pi-1} \varphi_i^T \varphi_i \leq \beta_2 I < \infty, \tag{3.13}$$

the adaptive residual generator is exponentially stable, and the parameter estimation $\widehat{\theta}_k$ converges to the true value θ with an exponential convergence rate:

$$\lim_{k\to\infty} \widehat{\theta}_k = \theta. \tag{3.14}$$

Proof. The proof can be found in the earlier study by Ding et al. [19, 20]. □

Until now, the unknown parameter θ has been assumed constant. We would like to further consider the behavior of the adaptive residual generator (3.5)–(3.10) in case θ is a time-varying parameter and bounds by (3.4). To simplify the notations, define

$$\eta_k = \widetilde{z}_k - V_k\widetilde{\theta}_k, \qquad \widetilde{z}_k = z_k - \widehat{z}_k, \qquad \widetilde{\theta}_k = \theta_k - \widehat{\theta}_k. \tag{3.15}$$

After a straightforward calculation, it follows that

$$\eta_{k+1} = \overline{A}_z\eta_k + \epsilon_k, \tag{3.16}$$

$$\widetilde{\theta}_{k+1} = \left(I - \gamma_k\varphi_k^T\varphi_k\right)\widetilde{\theta}_k + \overline{\epsilon}_k, \tag{3.17}$$

$$r_k = c_z\eta_k + \varphi_k\widetilde{\theta}_k, \tag{3.18}$$

with $\Theta_k = -\gamma_k\varphi_k^T c_z$, $\Delta_k = \theta_{k+1} - \theta_k$, $\overline{\epsilon}_k = \Theta_k\eta_k + \Delta_k$, and $\epsilon_k = -V_{k+1}\Delta_k$. According to (3.18), the residual r_k has a nonzero value since $\Delta_k \neq 0$. Assume that persistent excitation condition (3.13) is satisfied, the properties of adaptive residual generator (3.5)–(3.10) can be generalized in the following theorem.

Theorem 3.2. *In case of $\Delta_k \neq 0$ and bounded by* (3.4)*, the adaptive residual generator* (3.5)–(3.10) *ensures the following:*

(i) the estimation error $\widetilde{\theta}_k$ converges exponentially to the set

$$\mathcal{B} = \left\{\widetilde{\theta}_k \mid \left\|\widetilde{\theta}_k\right\| \leq \alpha_1^{k-k_0}\left\|\widetilde{\theta}_{k_0}\right\| + \frac{1-\alpha_1^{k-k_0}}{1-\alpha_1}\overline{\epsilon}\right\}, \quad 0 < \alpha_1 < 1, \tag{3.19}$$

where $\overline{\epsilon}$ is a positive scalar such that $\|\overline{\epsilon}_k\| < \overline{\epsilon}$ and k_0 denotes the initial time sample;

(ii) the residual signal r_k converges exponentially to the set

$$\mathcal{R} = \left\{r_k \mid |r_k| \leq \epsilon + \|\varphi_k\|\alpha_1^{k-k_0}\left\|\widetilde{\theta}_{k_0}\right\| + \|\varphi_k\|\frac{1-\alpha_1^{k-k_0}}{1-\alpha_1}\overline{\epsilon}\right\}, \tag{3.20}$$

where ϵ is a positive scalar such that $\|\epsilon_k\| < \epsilon$;

(iii) based on the assumption of the zero initial condition, that is, $\widetilde{\theta}_{k_0} = 0$, the normalized residual signal $\overline{r}_k$ satisfies

$$|\overline{r}_k| \leq \sqrt{s}v + \frac{1+\sqrt{s}}{1-\alpha_1}v, \tag{3.21}$$

where $\overline{r}_k = r_k/\sqrt{\delta + \varphi_k\varphi_k^T}$. *Furthermore, if the process corrupted by noise/disturbance, the residual signal can be formulated as*

$$r_k = c_z\eta_k + \varphi_k\widetilde{\theta}_k + p_k, \tag{3.22}$$

where p_k *represents the influence of noise/disturbance on the residual signal. It follows that*

$$|\overline{r}_k| \le \sqrt{s}v + \frac{1+\sqrt{s}}{1-\alpha_1}v + p, \tag{3.23}$$

with $p = \sup_{\forall k}(p_k/\sqrt{\delta + \varphi_k\varphi_k^T})$.

Proof. According to (3.17), for all $k > k_0$, we have

$$\widetilde{\theta}_k = S_{k,k_0}\widetilde{\theta}_{k_0} + \sum_{i=k_0}^{k-1} S_{k,i+1}\overline{\epsilon}_k, \tag{3.24}$$

where S_{k,k_0} is the transition matrix of the linear time-varying system (3.17). Since (3.13) is satisfied, the system (3.17) is exponentially stable; and Astrom and Wittenmark [27]. Therefore, there exists a positive constant $0 < \alpha_1 < 1$ such that $\|S_{k,k_0}\| \le \alpha_1^{k-k_0}$. Consequently, from (3.17), we have

$$\left\|\widetilde{\theta}_k\right\| \le \alpha_1^{k-k_0}\left\|\widetilde{\theta}_{k_0}\right\| + \left\|\sum_{i=k_0}^{k-1} S_{k\cdot i+1}\overline{\epsilon}_k\right\| \le \alpha_1^{k-k_0}\left\|\widetilde{\theta}_{k_0}\right\| + \frac{1-\alpha_1^{k-k_0}}{1-\alpha_1}\overline{\epsilon}. \tag{3.25}$$

Since $L_0 = 0$, $\overline{A}_z = A_z$, and all the eigenvalues of $\overline{A}_z$ are zero, it follows from (3.16) that

$$\left\|\eta_k\right\| \le \epsilon. \tag{3.26}$$

The bound of residual signal can be straightforwardly obtained

$$|r_k| \le \left\|c_z\eta_k\right\| + \left\|\varphi_k\widetilde{\theta}_k\right\| \le \epsilon + \left\|\varphi_k\right\|\alpha_1^{k-k_0}\left\|\widetilde{\theta}_{k_0}\right\| + \left\|\varphi_k\right\|\frac{1-\alpha_1^{k-k_0}}{1-\alpha_1}\overline{\epsilon}. \tag{3.27}$$

It is easier to prove that

$$\begin{aligned} \frac{\|\varepsilon_k\|}{\sqrt{\delta + \varphi_k\varphi_k^T}} &\le \sqrt{s}\|\Delta_k\| \le \sqrt{s}v, \\ \|\overline{\varepsilon}_k\| &\le \left(1+\sqrt{s}\right)\|\Delta_k\| \le \left(1+\sqrt{s}\right)v. \end{aligned} \tag{3.28}$$

Thus, set

$$\frac{\varepsilon}{\sqrt{\delta + \varphi_k \varphi_k^T}} = \sqrt{s}v, \qquad \bar{\epsilon} = \left(1 + \sqrt{s}\right)v, \tag{3.29}$$

the normalized residual becomes

$$|\bar{r}_k| \leq \sqrt{s}v + \frac{1 + \sqrt{s}}{1 - \alpha_1}v. \tag{3.30}$$

Equations (3.22)-(3.23) can be easily proved, and thus they are omitted here. □

According to Theorem 3.2, in case θ is a time-varying parameter and bounds by (3.4) the residual $\bar{r}_k$ is bounded and the threshold J_{th} can be set as the right-hand side presented by (3.23); that is,

$$J_{\text{th}} = \sqrt{s}v + \frac{1 + \sqrt{s}}{1 - \alpha_1}v + p. \tag{3.31}$$

The fault detection logic is given by

$$\begin{aligned} &|\bar{r}_k| \leq J_{\text{th}}, \quad \text{fault free,} \\ &|\bar{r}_k| > J_{\text{th}}, \quad \text{alarm for fault.} \end{aligned} \tag{3.32}$$

Remark 3.3. It is of great interest to detect the faults that cause abnormal changes on physical parameters of the process. Although the identified parameter θ is physically meaningless, any abnormal physical parameters variations can influence θ and should be finally discovered by the residual signal. In practice, the bound of normal variation rate of θ given by (3.4) can be determined through the offline test data. The related threshold of residual signal is designed for the detection of abnormal parameter change, which is supposed to be faster than the normal parameter variation.

Remark 3.4. The order of residual generator s could be significantly smaller than system order n in multiple output systems ($m > 1$): $s = (n + 1)/m - 1$. An algorithm is proposed in Ding et al. [19, 20] for constructing the reduced order residual generator. Thus, if persistent excitation condition is satisfied, the estimation error $\tilde{\theta}_k$ converges exponentially to a set determined by Δ_k. For industrial process, the excitation mainly comes from the variation of process variables and measurement noise.

Remark 3.5. Another efficient way to determine the threshold for residual signal is based on statistical methods. Without special assumption on process data, the so-called kernel density estimation (KDE) is widely used in practice for estimating the probability density function of residual signals. Based on a large number of offline test data, a proper threshold can be chosen under given confidence level. More detailed description on KDE can be found in Silverman [28] and Martin and Morris [29].

3.2. Fault Isolation Scheme Design

In this subsection, the fault isolation scheme will be further introduced in the framework of adaptive residual generator.

Suppose that there exist S classes of faults in the process including all potential abnormalities in sensors and actuators. Under the influence of ith class of fault, $i = 1, \ldots, S$, the unknown parameter becomes θ_f^i, which is assumed to belong to a known compact and convex set $\Theta_f^i \in \mathcal{R}^{s(m+l)+m}$. Note that, the set Θ_f^i could be offline identified by using the faulty data within the framework of adaptive scheme (3.5)–(3.10).

The proposed fault isolation strategy can be developed by integrating the fault information, that is, Θ_f^i. Based on it, S fault isolation observers are constructed, in which the ith observer is only responsible for the ith set of fault. According to the fault detection scheme discussed in the last subsection, after a fault is detected at time t_d, the fault isolation scheme is activated, such that the ith isolator is insensitive to the ith type of fault, but sensitive to other faults; see Zhang et al. [30]. In order to realize these requirements, the parameter projection method is utilized and the ith fault isolation observer has the following form:

$$\hat{z}_{k+1}^i = \overline{A}_z \hat{z}_k^i + Q(u_k, y_k)\hat{\theta}_k^i + V_{k+1}^i\left(\hat{\theta}_{k+1}^i - \hat{\theta}_k^i\right), \tag{3.33}$$

$$r_k^i = \hat{g}_k^i y_k - c_z \hat{z}_k^i,$$

$$V_{k+1}^i = \overline{A}_z V_k^i + Q(u_k, y_k) \in \mathcal{R}^{s\times[s(m+l)+m]}, \tag{3.34}$$

$$\varphi_k^i = c_z V_k^i - \begin{bmatrix} 0 & \cdots & 0 & y_k^T \end{bmatrix} \in \mathcal{R}^{s(m+l)+m},$$

$$\hat{\theta}_{k+1}^{i*} = \hat{\theta}_k^i + \frac{(\varphi_k^i)^T r_k^i}{\delta + \varphi_k^i (\varphi_k^i)^T} \in \mathcal{R}^{s(m+l)+m}, \tag{3.35}$$

$$\hat{\theta}_{k+1}^i = p_{\Theta_f^i}\left[\hat{\theta}_{k+1}^{i*}\right], \tag{3.36}$$

where

$$\hat{\theta}_k^i = \begin{bmatrix} \overline{\theta}_k^i \\ (\hat{g}_k^i)^T \end{bmatrix}, \quad \overline{\theta}_k^i \in \mathcal{R}^{s(m+l)},\ \hat{g}_k^i \in \mathcal{R}^m, \tag{3.37}$$

the $\delta > 0$, $p_{\Theta_f^i}$ denotes a projection operator that ensures $\hat{\theta}_{k+1}^i$ lies in a known bounded convex subset $\Theta_f^i \in \mathcal{R}^{s(m+l)+m}$. Details on the projection operator can be founded in Tao [26]. The following theorem states the properties of the ith isolation observer in case of the ith type of fault occurred.

Theorem 3.6. *Given the ith fault isolation observer in the form* (3.33)–(3.36)*, suppose that there is a positive constant d_i, such that for all $\theta_1, \theta_2 \in \Theta_f^i$, it follows that*

$$d_i = \sup_{\theta_1, \theta_2 \in \Theta_f^i} \|\theta_1 - \theta_2\|. \tag{3.38}$$

In case of the ith type of fault occurs, one has the following:

(i) the ith fault isolation observer is stable and

$$\left\|\widetilde{\theta}_{k+1}^{i}\right\| \le d_i, \qquad \left\|\widehat{\theta}_{k+1}^{i} - \widehat{\theta}_{k}^{i}\right\| \le \left|\overline{r}_k^i\right|, \tag{3.39}$$

where $\overline{r}_k^i = r_k^i / \sqrt{\delta + \varphi_k^i (\varphi_k^i)^T}$, $\widetilde{\theta}_{k+1}^{i} = \theta_{k+1}^{i} - \widehat{\theta}_{k+1}^{i}$,

(ii) based on the assumption of the zero initial condition, the normalized residual signal satisfies

$$\left(\overline{r}_k^i\right)^2 \le d_i^2 + \left(2s + 2\sqrt{s} + 1\right) v_i^2 + \left(2 + 2\sqrt{s}\right) v_i d_i, \tag{3.40}$$

where v_i *is a positive scalar such that* $\|\Delta_k^i\| \le v_i$ *with* $\Delta_k^i = \theta_{k+1}^{i} - \theta_k^i$.

Proof. According to the property of the projection operator, it follows that $\widehat{\theta}_{k+1}^{i} \in \Theta_f^i$. From (3.38), we have

$$\left\|\widetilde{\theta}_{k+1}^{i}\right\| = \left\|\theta_{k+1}^{i} - \widehat{\theta}_{k+1}^{i}\right\| \le d_i. \tag{3.41}$$

It is evident that for all k,

$$\left\|\widehat{\theta}_{k+1}^{i} - \theta_{k+1}^{i}\right\| \le \left\|\widehat{\theta}_{k+1}^{i*} - \theta_{k+1}^{i}\right\|, \tag{3.42}$$

and consequently,

$$\left\|\widehat{\theta}_{k+1}^{i} - \widehat{\theta}_{k}^{i}\right\| \le \left\|\widehat{\theta}_{k+1}^{i*} - \widehat{\theta}_{k}^{i}\right\| \le \frac{\left\|(\varphi_k^i)^T\right\| \left|\overline{r}_k^i\right|}{\delta + \varphi_k^i (\varphi_k^i)^T} \le \left|\overline{r}_k^i\right|. \tag{3.43}$$

Now, define a new parameter

$$\widetilde{\theta}_{k+1}^{i*} = \widehat{\theta}_{k+1}^{i*} - \theta_{k+1}^{i}. \tag{3.44}$$

Using (3.42), we get

$$\left\|\widetilde{\theta}_{k+1}^{i}\right\|^2 - \left\|\widetilde{\theta}_{k}^{i}\right\|^2 \le \left\|\widetilde{\theta}_{k+1}^{i*}\right\|^2 - \left\|\widetilde{\theta}_{k}^{i}\right\|^2. \tag{3.45}$$

The right-hand side of (3.45) becomes

$$\left\|\widetilde{\theta}_{k+1}^{i*}\right\|^2 - \left\|\widetilde{\theta}_{k}^{i}\right\|^2 = \left(\theta_{k+1}^{i} - \widehat{\theta}_{k+1}^{i*} - \theta_k^i + \widehat{\theta}_k^i\right)^T \left(\theta_{k+1}^{i} - \widehat{\theta}_{k+1}^{i*} + \theta_k^i - \widehat{\theta}_k^i\right). \tag{3.46}$$

Note that, (3.35) can be reformulated as

$$\widehat{\theta}_{k+1}^{i*} = \widehat{\theta}_k^i + \left(\overline{\varphi}_k^i\right)^T \overline{r}_k^i, \tag{3.47}$$

where

$$\left(\overline{\varphi}_k^i\right)^T = \frac{\left(\varphi_k^i\right)^T}{\sqrt{\delta + \varphi_k^i \left(\varphi_k^i\right)^T}}. \tag{3.48}$$

For the normalized residual signal $\overline{r}_k^i$, it is known that

$$\overline{r}_k^i = \overline{\varphi}_k^i \widetilde{\theta}_k^i + \overline{\eta}_k^i, \tag{3.49}$$

with

$$\begin{aligned} \overline{\eta}_k^i &= \frac{c_z \eta_k^i}{\sqrt{\delta + \varphi_k^i \left(\varphi_k^i\right)^T}}, \\ \eta_k^i &= \overline{A}_z \eta_{k-1}^i - V_k^i \Delta_{k-1}^i, \\ \Delta_{k-1}^i &= \theta_k^i - \theta_{k-1}^i, \quad 0 \le \overline{\varphi}_k \overline{\varphi}_k^T \le 1. \end{aligned} \tag{3.50}$$

Combining (3.46), (3.47), and (3.49), we have

$$\left\|\widetilde{\theta}_{k+1}^i\right\|^2 - \left\|\widetilde{\theta}_k^i\right\|^2 \le -\left(\overline{r}_k^i\right)^2 + 2\overline{r}_k^i \overline{\eta}_k^i + \left(-2\overline{\varphi}_k^i \overline{r}_k^i + 2\left(\widetilde{\theta}_k^i\right)^T + \left(\theta_{k+1}^i\right)^T - \left(\theta_k^i\right)^T\right) \Delta_k^i. \tag{3.51}$$

Equation (3.51) can be reformulated as

$$\left(\overline{r}_k^i\right)^2 \le -\left\|\widetilde{\theta}_{k+1}^i\right\|^2 + \left\|\widetilde{\theta}_k^i\right\|^2 + 2\left(\overline{\eta}_k^i\right)^2 + 2\left|\overline{\eta}_k^i\right| \left\|\widetilde{\theta}_k^i\right\| \tag{3.52}$$

$$+ \left\|\theta_{k+1}^i - \theta_k^i\right\| \left(2\left\|\widetilde{\theta}_k^i\right\| + 2\left|\overline{\eta}_k^i\right| + \left\|\theta_{k+1}^i - \theta_k^i\right\|\right). \tag{3.53}$$

Since

$$\left|\overline{\eta}_k^i\right| \le \frac{\left\|\eta_k^i\right\|}{\sqrt{\delta + \varphi_k^i \left(\varphi_k^i\right)^T}} \le \sqrt{s} v_i, \tag{3.54}$$

according to (3.52), the result represented by (3.40) can be easily proved. □

For the ith isolation observer, define the fault isolation index

$$J_k^i = \overline{r}_k^i, \tag{3.55}$$

and the related threshold $J_{\text{th}}^{i,\text{iso}}$. Based on Theorem 3.6, we have the following corollary.

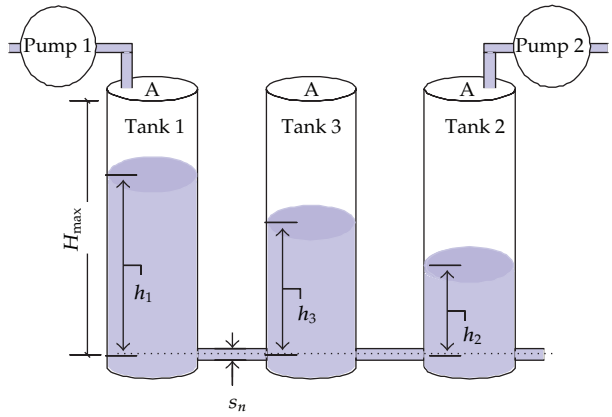

Figure 1: Structure of TTS.

Corollary 3.7. *For the ith isolation observer, the fault isolation threshold $J_{th}^{i,iso}$ can be determined by*

$$J_{th}^{i,iso} = \sqrt{d_i^2 + (2s + 2\sqrt{s} + 1)v_i^2 + (2 + 2\sqrt{s})v_i d_i}. \tag{3.56}$$

Moreover, if the process corrupted by disturbance and/or noise, the normalized residual is

$$\overline{r}_k^i = \overline{\varphi}_k^i \widetilde{\theta}_k^i + \overline{\eta}_k^i + \overline{p}_k^i, \tag{3.57}$$

where $\overline{p}_k^i$ represents the influence of noise/disturbance on the normalized residual signal. In this case, the threshold for fault isolation purpose is given by

$$J_{th}^{i,iso} = \sqrt{d_i^2 + (2s + 2\sqrt{s} + 1)v_i^2 + cv_i d_i + c\overline{p}^i v_i}, \tag{3.58}$$

with

$$\overline{p}^i = \sup_{\forall k}\left(\overline{p}_k^i\right), \qquad c = 2 + 2\sqrt{s}. \tag{3.59}$$

Proof. The proof is straightforward based on Theorem 3.6 and omitted here. □

The fault isolation logic can be described as the following:

(i) for the ith isolation observer, if $\exists t_a > t_d$ such that $|J_{t_a}^i| > J_{\text{th}}^{i,\text{iso}}$, then the occurrence of the ith type of fault is excluded;

(ii) otherwise, if $|J_{t_a}^i| < J_{\text{th}}^{i,\text{iso}}$ for $\forall t_a > t_d$, the ith type of fault is occurred.

The sufficient condition of fault isolability is given by the following theorem.

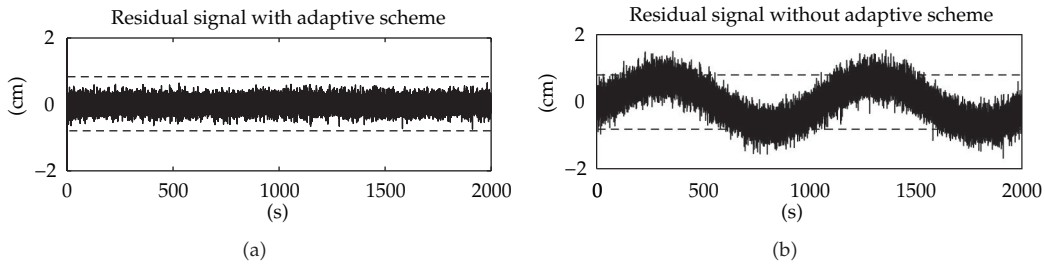

Figure 2: Residual signal.

Theorem 3.8. *Based on the fault isolation observer* (3.33)–(3.36)*, the* i*th type of fault, which detected at time* t_d*, is isolable, if for the other* $S-1$ *fault isolation observers,* $\exists t_a > t_d$ *such that the following inequality is satisfied*

$$\left|\overline{\varphi}_{t_a}^r \widetilde{\theta}_{t_a}^r\right| > \sqrt{s} v_r + \sqrt{s v_r^2 + \left(J_{th}^{r,iso}\right)^2}, \tag{3.60}$$

where

$$J_{\text{th}}^{r,iso} = \sqrt{d_r^2 + \left(2s + 2\sqrt{s} + 1\right) v_r^2 + \left(2 + 2\sqrt{s}\right) v_r d_r}, \quad r = 1, \ldots, S,\ r \neq i. \tag{3.61}$$

Furthermore, if $s = 1$, $L_0 = 0$*, it follows that*

$$\left|\overline{\varphi}_{t_a}^r \widetilde{\theta}_{t_a}^r\right| > v_r + \sqrt{d_r^2 + 6v_r^2 + 4v_r d_r}. \tag{3.62}$$

Proof. For the rth fault isolation observer, we have

$$\begin{aligned} \left(J_{t_a}^r\right)^2 &= \left(\overline{\varphi}_{t_a}^r \widetilde{\theta}_{t_a}^r\right)^2 + \left(\overline{\eta}_{t_a}^r\right)^2 + 2\overline{\varphi}_{t_a}^r \widetilde{\theta}_{t_a}^r \overline{\eta}_{t_a}^r \\ &\geq \left(\overline{\varphi}_{t_a}^r \widetilde{\theta}_{t_a}^r\right)^2 - 2\sqrt{s} v_r \left|\overline{\varphi}_{t_a}^r \widetilde{\theta}_{t_a}^r\right|. \end{aligned} \tag{3.63}$$

Straightforwardly, if for all $r = 1, \ldots, S,\ r \neq i$, $\exists t_a > t_d$ such that

$$\left(\overline{\varphi}_{t_a}^r \widetilde{\theta}_{t_a}^r\right)^2 - 2\sqrt{s} v_r \left|\overline{\varphi}_{t_a}^r \widetilde{\theta}_{t_a}^r\right| > \left(J_{\text{th}}^{r,\text{iso}}\right)^2, \tag{3.64}$$

the ith type of fault is isolable and directly (3.60) is proofed. In the case of $s = 1$ and $L_0 = 0$, (3.62) is straightforward. □

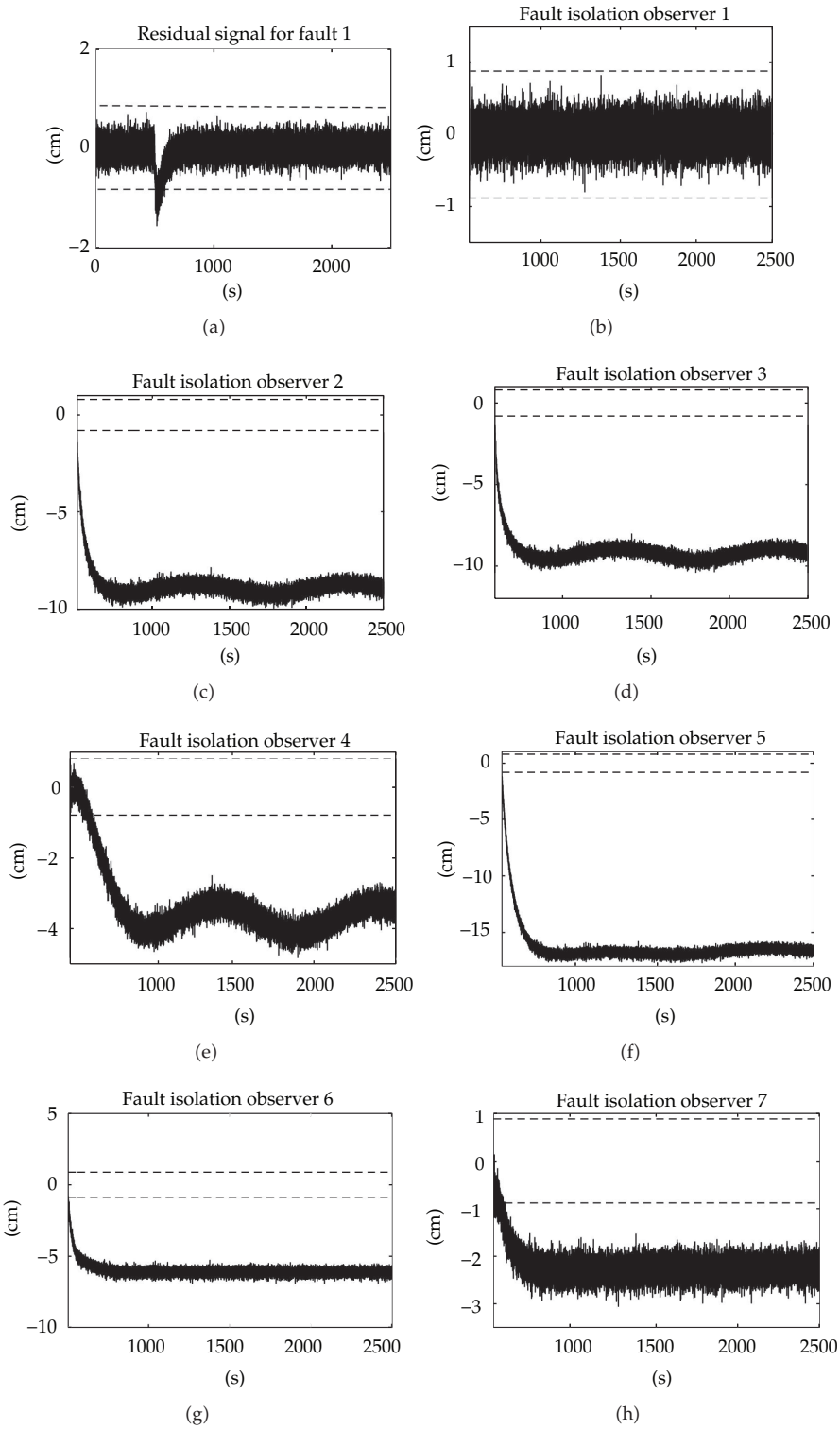

Figure 3: Continued.

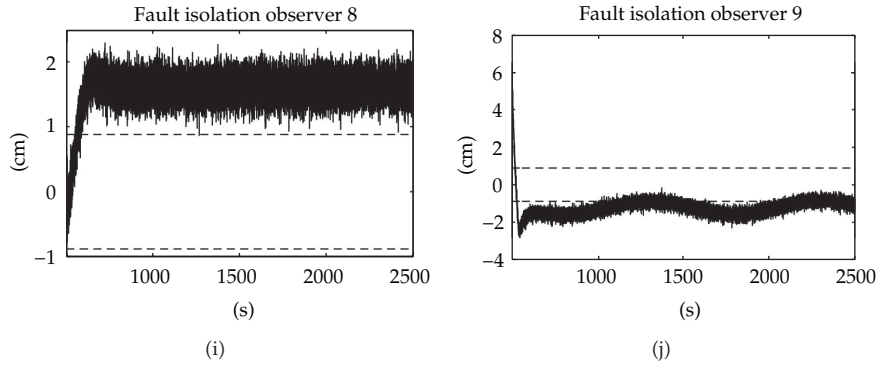

Figure 3: Fault diagnosis for fault 1.

4. Application to Three-Tank System

The three-tank system (TTS) considered in our study is a laboratory setup located in the laboratory of Institute for Automatic Control and Complex Systems, University of Duisburg-Essen. The sketch is shown in Figure 1, which has typical characteristics of tanks, pipelines, and pumps used in the chemical industry and thus often serves as benchmark process for many control and monitoring relevant studies.

The plant consists of three cylindrical tanks which are serially interconnected with each other by cylindrical pipes with the cross-section of S_n. The outflowing water is collected in a reservoir, which supplies pumps 1 and 2. $H_{\max}$ denotes the maximal height of tanks. The flow rates and water levels of tanks, represented by h_i, $i = 1, 2, 3$, are measured throughout the process. By integrating a nonlinear controller, water levels h_1 and h_2 can be controlled. The detailed description of TTS can be found in Ding [6].

It is well known that the system matrices of TTS, which are achieved from linearization at different operation points, are different. In our experiment, the operation point of water level h_1 is periodically changed in order to simulate the normal parameter variations in the process. An experiment including the following steps has been performed.

(i) Place TTS at the operating point $h_1 = 35 + \sin(0.002t)$ cm, $h_2 = 25$ cm, in which sin signal added to h_1 leads to normal parameter variations.

(ii) Use the adaptive scheme (3.5)–(3.10) to identify θ through the data collected at the operating point $h_1 = 35$ cm, $h_2 = 25$ cm with reduced order $s = 1$ and $L_0 = 0$. Note that the system order $n = 3$ can be determined by Algorithm D2PS, and based on it the reduced order s is calculated according to the relationship $s = (n + 1)/m - 1$ with two system outputs; that is, $m = 2$.

(iii) Construct two residual generators: (a) an adaptive residual generator (3.5)–(3.10) (b) a standard one without adaptive scheme.

(iv) Both the residual generators run for 2000 s (seconds). The threshold $J_{\text{th}} = 0.78$ is determined according to (3.23) with the parameters $\mu = 0.01$, $\alpha_1 = 0.9997$, $v = 7.3668 \times 10^{-5}$, and $p = 0.55$, which are chosen according to the offline test data.

Figure 2 shows the residual signals with and without the adaptive scheme. It is clear that the standard process monitoring method is unsuitable to monitor TTS with normal parameters variations that is apparent by the numerous false alarms.

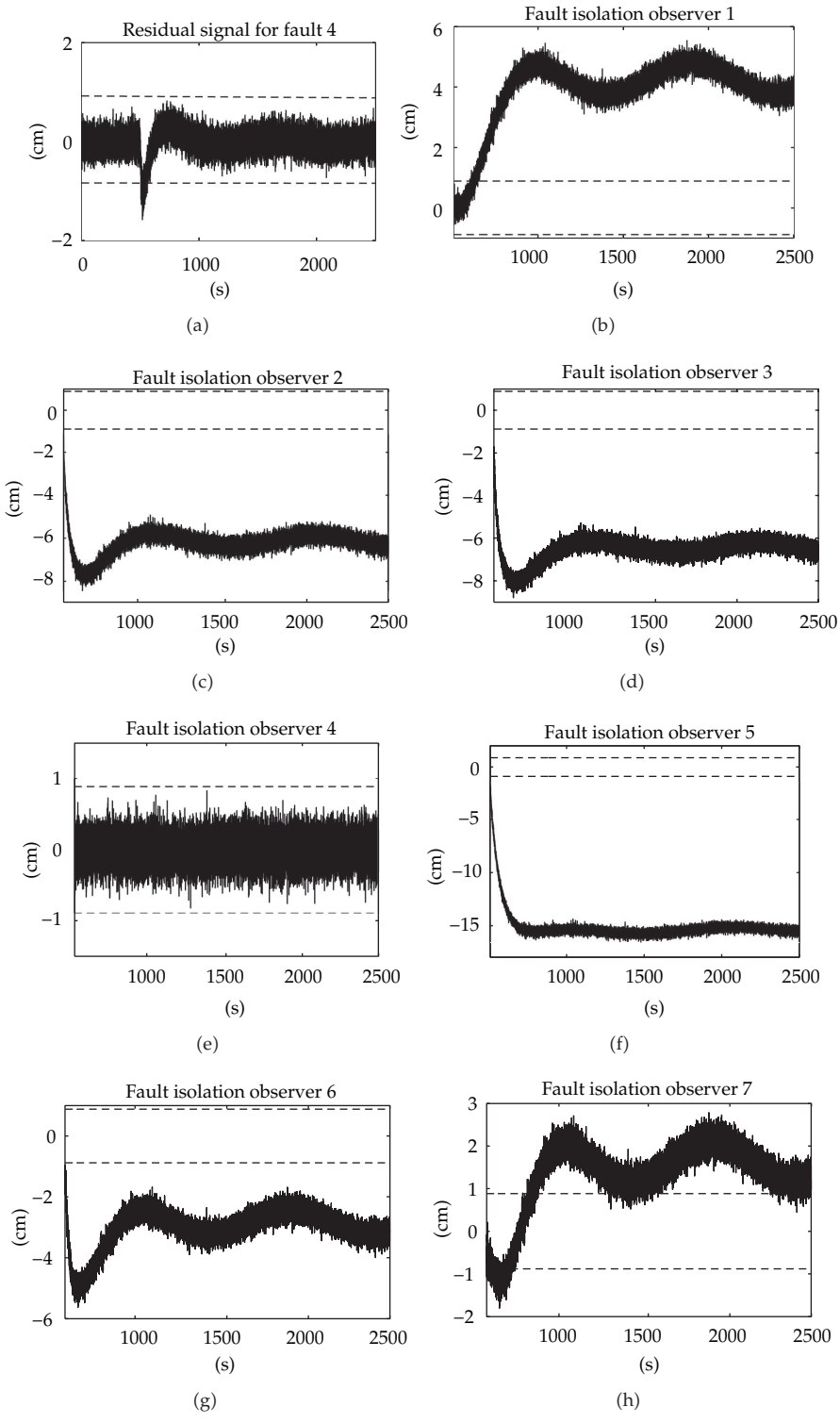

Figure 4: Continued.

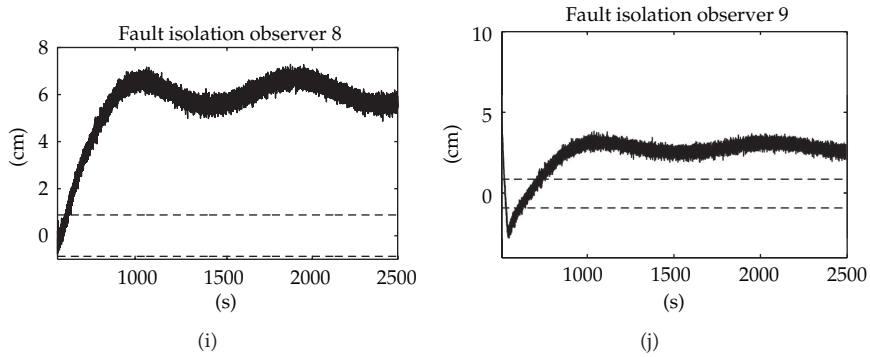

(i) (j)

Figure 4: Fault diagnosis for fault 4.

Table 1: The faults existed in TTS.

Fault number	Description	Type
Faults 1–3	Leaking in tank 1, 2, 3	Process fault
Faults 4-5	Offset of actuator Q_1, Q_2	Actuator fault
Faults 6–8	Plugging in tank 1, 2, 3	Process fault
Fault 9	Offset of sensor h_1	Sensor fault

The faults occurred in TTS can be classified as process fault, sensor fault, and actuator fault, which are shown in Table 1. To verify the performance of the proposed fault diagnosis scheme, the following experiment is carried out.

(i) Offline: apply adaptive scheme (3.5)–(3.10) to identify Θ_f^i through the ith type of faulty data with $s = 1$ and $L_0 = 0$.

(ii) Online: use adaptive residual generator (3.5)–(3.10) for fault detection purpose. If there exists time t_d such that $|\overline{r}_k| > J_{th}$, the alarm is released. Simultaneously, the $S-1$ fault isolation observers (3.33)–(3.36) are activated, and the threshold $J_{\text{iso}}^i = 0.8822$ is determined according to (3.58) with the parameters $v_i = 1 \times 10^{-2}$, $d_i = 0.85$, and $\overline{p}_i = 0.55$.

The fault diagnosis results of faults 1, 4, and 9, which represent the process, actuator, and sensor fault, are mainly presented in the following study. All these faults occur at the 500th second. The sensor fault 9 has 30% offset compared to the normal value and the actuator fault 4 represents 100% offset to the desired value. Figures 3(a), 4(a), and 5(a) show the residual signal from adaptive residual generator for fault detection purpose. It can be seen that the faults are successfully detected at the 505 s, the 507 s, and the 501 s, respectively.

In the meanwhile, the fault isolation observers are activated, and the related fault isolation indices are shown in Figures 3(b)–3(j), 4(b)–4(j), and 5(b)–5(j) for faults 1, 4, 9, respectively. It is evident that the fault isolation indices from the 1st isolation observer (Figure 3(b)), the 4th isolation observer (Figure 4(e)), and the 9th isolation observer (Figure 5(j)) are consistently maintained under respective thresholds which indicate occurrence of these faults. On the other hand, the other subfigures show the isolation indices associated to other isolation observers. It is obvious that all of them exceed the related thresholds, which indicate the absence of these faults in the process.

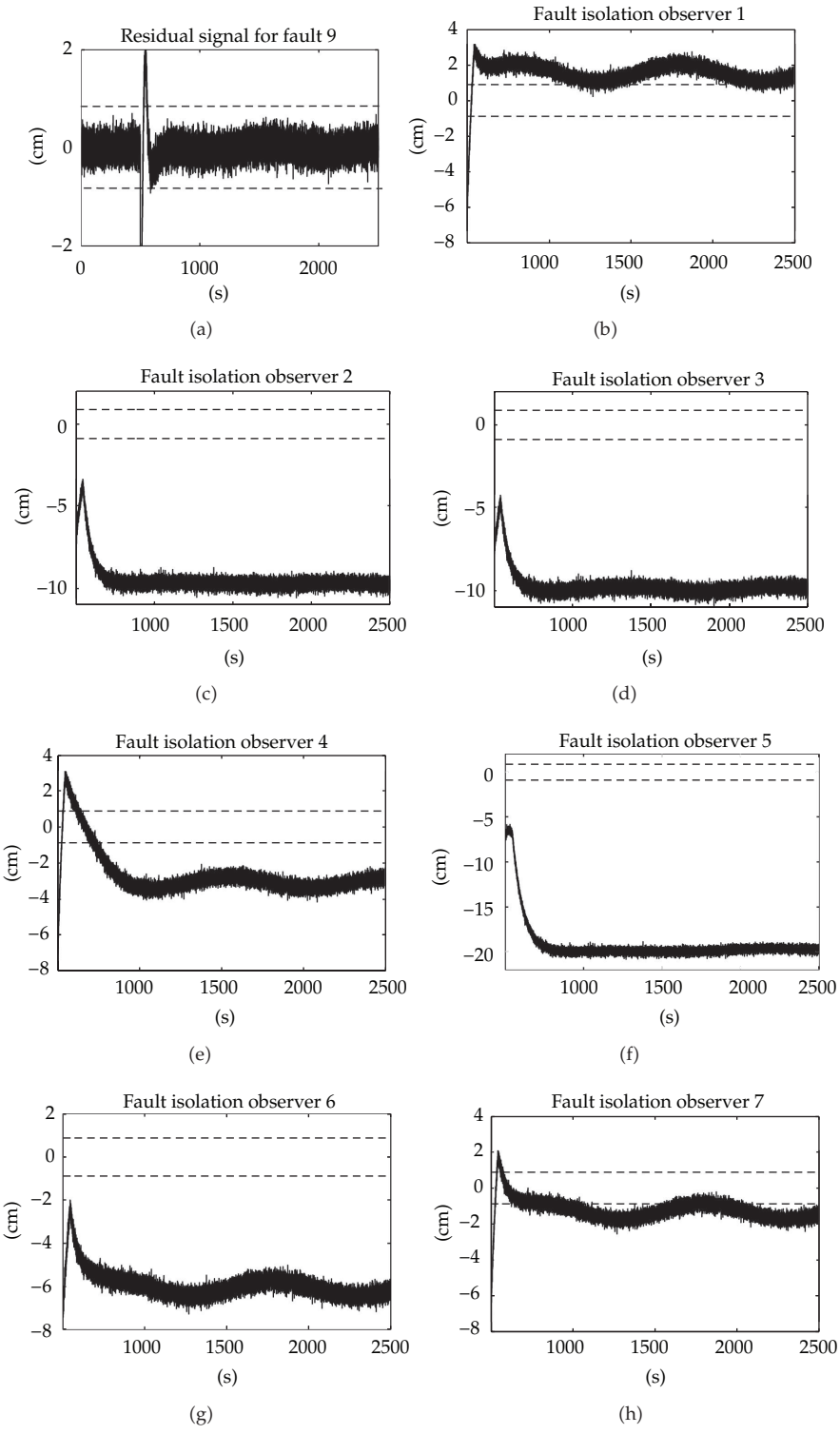

Figure 5: Continued.

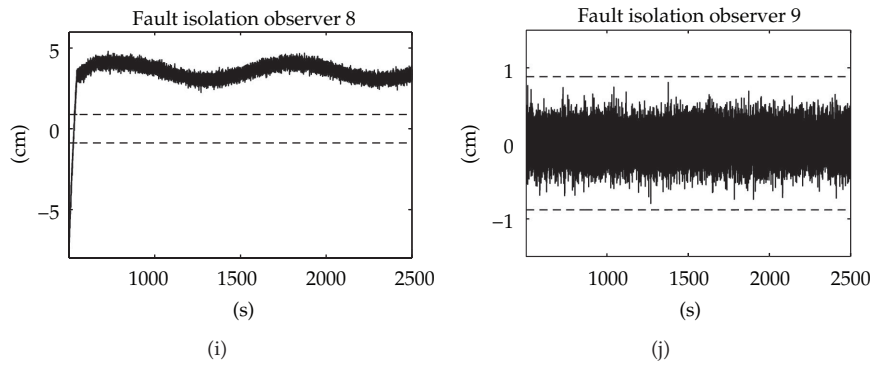

Figure 5: Fault diagnosis for fault 9.

5. Conclusion

In this paper, we have proposed an approach for data-driven design of fault diagnosis system, which consists of an adaptive residual generator and a bank of observers for fault detection and isolation purposes. Analytical results regarding the issues of adaptive observers, threshold calculation, and fault isolation strategy are discussed. The proposed design scheme is demonstrated on the simulation of laboratory-scale three-tank system, which shows satisfactory fault diagnosis performance.

References

[1] J. Gertler, *Fault Detection and Diagnosis in Engineering Systems*, Marcel Dekker, New York, NY, USA, 1998.

[2] J. Chen and R. Patton, *Robust Model-Based Fault Diagnosis for Dynamic Systems*, Kluwer Academic, Norwell, Mass, USA, 1999.

[3] R. Patton, P. Frank, and R. Clark, *Issues of Fault Diagnosis for Dynamic Systems*, Springer, Berlin, Germany, 2000.

[4] M. Blanke, M. Kinnaert, J. Lunze, M. Staroswiecki, and J. Schröder, *Diagnosis and Fault-Tolerant Control*, Springer, Berlin, Germany, 2006.

[5] R. Isermann, *Fault Diagnosis Systems: An Introduction from Fault Detection to Fault Tolerance*, Springer, Berlin, Germany, 2006.

[6] S. Ding, *Model-Based Fault Diagnosis Techniques*, Springer, Berlin, Germany, 2008.

[7] L. Ljung, *System Identification: Theory for the User*, Prentice Hall, Englewood Cliffs, NJ, USA, 1987.

[8] P. V. Overschee and B. D. Moor, *Subspace Identification for Linear Systems*, Kluwer Academic, Dordrecht, The Netherlands, 1996.

[9] W. Favoreel, B. De Moor, and P. Van Overschee, "Subspace state space system identification for industrial processes," *Journal of Process Control*, vol. 10, no. 2-3, pp. 149–155, 2000.

[10] S. Qin, "An overview of subspace identification," *Computers and Chemical Engineering*, vol. 30, no. 10–12, pp. 1502–1513, 2006.

[11] I. Hwang, S. Kim, Y. Kim, and C. E. Seah, "A survey of fault detection, isolation, and reconfiguration methods," *IEEE Transactions on Control Systems Technology*, vol. 18, no. 3, pp. 636–653, 2010.

[12] V. Venkatasubramanian, R. Rengaswamy, K. Yin, and S. Kavuri, "A review of process fault detection and diagnosis. Part I: Quantitative model-based methods," *Computers and Chemical Engineering*, vol. 27, pp. 293–311, 2003.

[13] P. Zhang and S. Ding, "On fault detection in linear discrete-time, periodic, and sampled-data systems (survey)," *Journal of Control Science and Engineering*, vol. 2008, Article ID 849546, 19 pages, 2008.

[14] B. Shen, Z. Wang, H. Shu, and G. Wei, "Robust $H\infty$ finite-horizon filtering with randomly occurred nonlinearities and quantization effects," *Automatica*, vol. 46, no. 11, pp. 1743–1751, 2010.

[15] B. Shen, Z. Wang, and Y. S. Hung, "Distributed $H\infty$-consensus filtering in sensor networks with multiple missing measurements: the finite-horizon case," *Automatica*, vol. 46, no. 10, pp. 1682–1688, 2010.

[16] H. Dong, Z. Wang, D. W. C. Ho, and H. Gao, "Robust $H\infty$ filtering for Markovian jump systems with randomly occurring nonlinearities and sensor saturation: the finite-horizon case," *IEEE Transactions on Signal Processing*, vol. 59, no. 7, pp. 3048–3057, 2011.

[17] H. Dong, Z. Wang, J. Lam, and H. Gao, "Fuzzy-model-based robust fault detection with stochastic mixed time-delays and successive packet dropouts," *IEEE Transactions on Systems, Man, and Cybernetics*, vol. 42, no. 3, part B, pp. 365–376, 2012.

[18] S. X. Ding, P. Zhang, B. Huang, and E. L. Ding, "Subspace method aided data-driven design of observer based fault detection systems," in *Proceedings of the 16th Triennial World Congress of International Federation of Automatic Control (IFAC '05)*, pp. 167–172, Prague, Czech Republic, July 2005.

[19] S. Ding, S. Yin, P. Zhang, E. Ding, and A. Naik, "An approach to data-driven adaptive residual generator design and implementation," in *Proceedings of the 7th IFAC Symposium on Fault Detection and Supervision and Safety of Technical Processes*, Barcelona, Spain, 2009.

[20] S. X. Ding, P. Zhang, A. Naik, E. L. Ding, and B. Huang, "Subspace method aided data-driven design of fault detection and isolation systems," *Journal of Process Control*, vol. 19, no. 9, pp. 1496–1510, 2009.

[21] S. Yin, A. Naik, and S. Ding, "Data-driven design of fault diagnosis scheme for periodic systems," in *Proceedings of the 7th Workshop on Advanced Control and Diagnosis*, Zielona Gora, Poland, 2009.

[22] S. Ding, S. Yin, Y. Wang, Y. Wang, Y. Yang, and B. Ni, "Data-driven design of observers and its applications," in *Proceedings of the 18th IFAC World Congress*, Milano, Italy, 2011.

[23] S. Ding, P. Zhang, E. Ding, P. Engel, and W. Gui, "A survey of the application of basic data-driven and model-based methods in process monitoring and fault diagnosis," in *Proceedings of the 18th IFAC World Congress*, Milano, Italy, 2011.

[24] L. Chiang, E. Russell, and R. Braatz, *Fault Detection and Diagnosis in Industrial Systems*, Springer, London, UK, 2001.

[25] P. Ioannou and J. Sun, *Robust Adaptive Control*, Prentice Hall, 1996.

[26] G. Tao, *Adaptive Control Design and Analysis*, Wiley-Interscience, Hoboken, NJ, USA, 2003.

[27] K. Astrom and B. Wittenmark, *Adaptive Control*, Addison-Wesley, 1995.

[28] B. W. Silverman, *Density Estimation for Statistics and Data Analysis*, Chapman & Hall, London, UK, 1986.

[29] E. Martin and A. Morris, "Non-parametric confidence bounds for process performance monitoring charts," *Journal of Process Control*, vol. 6, no. 6, pp. 349–358, 1996.

[30] X. Zhang, M. Polycarpou, and T. Parisini, "Design and analysis of fault isolation scheme for a class of uncertain nonlinear systems," *Annual Reviews in Control*, vol. 32, pp. 107–121, 2008.